


Research Article

Modeling the Effect of the Platoon Size of CAVs on Mixed Traffic Flow: A Cellular Automaton Method

Yangsheng Jiang,^{1,2,3} Zhiyuan Yi,^{1,2} Guosheng Xiao,^{1,2} Hongwu Li,^{1,2,3}
and Zhihong Yao ^{1,2,3}

¹School of Transportation and Logistics, Southwest Jiaotong University, Chengdu, Sichuan 610031, China

²National Engineering Laboratory of Integrated Transportation Big Data Application Technology, Southwest Jiaotong University, Chengdu, Sichuan 611756, China

³National United Engineering Laboratory of Integrated and Intelligent Transportation, Southwest Jiaotong University, Chengdu, Sichuan 611756, China

Correspondence should be addressed to Zhihong Yao; zh Yao@swjtu.edu.cn

Received 19 July 2023; Revised 30 August 2023; Accepted 13 September 2023; Published 21 September 2023

Academic Editor: Jingda Wu

Copyright © 2023 Yangsheng Jiang et al. This is an open access article distributed under the Creative Commons Attribution License, which permits unrestricted use, distribution, and reproduction in any medium, provided the original work is properly cited.

This study proposes a cellular automaton model incorporating the platoon size of connected automated vehicles (CAVs) to examine their impact on mixed traffic flow. First, vehicles are classified into three modes, human-driven vehicles (HDVs), adaptive cruise control (ACC), and cooperative adaptive cruise control (CACC), by considering the characteristics of the car-following behavior. Second, the CACC is further subdivided into interplatoon and intraplatoon car-following modes due to the limitations of the platoon size of CAVs. Then, cellular automaton rules are developed for each of these four modes. Finally, numerical simulation experiments are conducted to analyze the influence of the penetration rate and platoon size of CAVs on mixed traffic flow. The results demonstrate that (1) the simulation results closely align with the theoretically derived outcomes, with an error rate of only 0.46% at a penetration rate of 100%; (2) when the penetration rate of CAVs reaches 100%, increasing the platoon size further enhances the traffic capacity; and (3) the optimal platoon size is determined to be seven CAVs under moderate traffic density.

1. Introduction

Autonomous vehicles are increasingly entering our range of vision as more advanced technologies are being used in vehicles, making them smarter and safer. In addition, connected and autonomous vehicles (CAVs) have emerged due to the development of 5G Internet technology. CAVs can gather complicated data, including nearby people and objects, road conditions, and traffic infrastructure, by using advanced sensors. Then, they interpret the information and deliver it to the driving control system. CAVs can also broadcast data about how their car operates to nearby vehicles. The Chinese government has devised the “Connected Automated Vehicle Technology Roadmap 2.0,” projecting that semiautonomous and conditionally autonomous vehicles will capture an

estimated 50% share of new car sales by 2025. Furthermore, highly CAVs will be widely deployed in various regions by 2035 [1, 2]. Due to the quick growth of connected automated technologies, there will be mixed traffic flows consisting of both CAVs and HDVs coexisting for a long time in the future [3–5]. Compared with traditional vehicles, through vehicle-to-vehicle (V2V) communication and vehicle-to-infrastructure (V2I) communication, CAVs can achieve real-time information sharing, thereby forming flexible vehicle fleets, which significantly improve road capacity and alleviate traffic congestion [6, 7]. Extensive research highlights the benefits of vehicle platooning, including a more compact vehicle arrangement, reduced human driving errors, and enhanced road traffic efficiency. Notably, the size of vehicle platoons assumes a pivotal role in effective platoon management [8–10]. Consequently,

a comprehensive investigation into the mixed traffic flow characteristics, considering the platoon size of CAVs, assumes paramount significance.

Cellular automaton has garnered significant attention in traffic flow research due to its computational efficiency and capacity to simulate intricate traffic phenomena by setting simple rules [11–15]. In the pursuit of understanding traffic flow dynamics, numerous scholars have employed cellular automaton models to capture the microlevel driving behaviors of vehicles within mixed traffic scenarios. As the intelligent connected technology continues to advance, researchers are expanding their focus beyond individual CAVs and exploring the formation of CAV platoons. However, in real-world scenarios, the size of the CAV platoons is often constrained by the limitations of the intervehicle communication range. Existing investigations have highlighted that once CAV platoons reach their maximum size, additional vehicles are precluded from joining the platoon, thus forming new platoons with more significant headways. Consequently, there is a pressing need for further research to model the following behavior between CAV platoons [16–19].

To address this gap, this study considers the platoon size when developing the cellular automaton model. By referring to references [20, 21], based on the characteristics of car-following behavior, the car-following modes on the road are classified into human-driven vehicles (HDV), adaptive cruise control (ACC), and cooperative adaptive cruise control (CACC). Accounting for the limitations of the platoon size, the CACC is further subdivided into intraplatoon and interplatoon car-following modes. Then, separate cellular automaton models are established for all four car-following modes. Subsequently, numerical simulation experiments are devised to comprehensively analyze the characteristics and sensitivity of mixed traffic flow. The main contributions of this paper are as follows:

- (1) CACC is subdivided into intraplatoon and interplatoon following modes to consider the limitation of platoon size. Then, cellular automaton models are established for the two following modes. This will better simulate the car-following behavior of CAV platoons in real road traffic flow.
- (2) We investigate the effects of the penetration rates of CAVs on mixed traffic flow, including fundamental diagrams, traffic congestion, and reaction time.
- (3) We evaluate the impact of platoon size on traffic capacity and determine the optimal platoon size for different traffic densities.

The remainder of this paper is organized as follows. Section 2 reviews the relevant work. Section 3 analyzes the driving characteristics of different car-following modes and establishes a cellular automaton model. Section 4 designs simulation experiments to study the impact of CAV penetration rate on traffic flow and determines the optimal platoon

size under different traffic densities. Finally, Section 5 concludes this study and proposes future research directions.

2. Literature Review

In 1992, Nagel and Schreckenberg [22] proposed an NS model capable of simulating simple traffic flow phenomena. Many scholars have made improvements on this basis. M. Takayasu and H. Takayasu [23] took the lead in introducing the slow-start rule into the NS model and proposed the TT model. The results show that the model can not only simulate metastable and hysteresis phenomena but also simulate the phenomenon of exit phase separation under high traffic density. Zeng et al. [24] redefined the object of stochastic slowdown and proposed the cruising driving limit model. Benjamin et al. [25] reformulated the slow start rule, leading to the development of the BJH model. Schreckenberg et al. [26] established a probabilistic relationship between stochastic slowdown and vehicle speed, giving rise to the VDR model. Furthermore, through improving the acceleration rules, several models have been proposed, including the comfortable driving model [27], the Fukui–Ishibashi model [28], the three-phase traffic flow model [29], and the optimal velocity model [30].

With the continuous development of intelligent and connected technology, many scholars have begun to study the mixed traffic flow of autonomous vehicles (AVs) and human-driven vehicles (HDVs). Regarding the traffic flow characteristics, Yang et al. [31] introduced the Gipps safe distance rule based on the NS model and used different reaction times to differentiate between AVs and HDVs. Through numerical simulation, they found that AVs can improve traffic capacity and alleviate traffic congestion. Seeking to delve deeper into the influence of vehicle reaction time on road traffic flow, Vranken et al. [32] devised a single-lane cellular automaton model with a fine time step of 0.1 s. This model incorporates a finite braking capacity and successfully eliminates velocity fluctuations when the CAVs penetration rate reaches 100%. Focusing on traffic safety considerations, Ye and Yamamoto [33] employed the frequency of hazardous situations and collision time as evaluative indicators to evaluate traffic flow safety. They investigated the impact of CAVs' penetration rates on traffic safety through simulations. The results demonstrated a notable improvement in traffic safety conditions as the prevalence of automated driving vehicles increased. Gong et al. [34] constructed a cellular automaton model that accounts for limited visibility, aiming to examine the influence of CAVs on road safety under extreme weather conditions. This study incorporated diverse car-following scenarios and systematically explored the effects of visibility levels and CAV penetration rates on traffic safety. The findings provide valuable insights into managing future mixed traffic flow in dense fog conditions. Regarding the intersection traffic control, Marzoug et al. [35] adopted an open boundary and proposed an equation for calculating the probability of accidents based on the NS model. The results showed that the probability of accidents exhibits three

different patterns as the CAV penetration rate changes. To further investigate the traffic control methods under the nonvehicle network intersections and interactions of the connected vehicles (CVs), Zhao et al. [36] considered vehicle-to-vehicle and vehicle-to-signal communication and proposed two cellular automaton models, namely, CE-NS and CI-NS. Factors such as preceding vehicle speed and signal conditions were adequately considered when setting the rules. The results indicated that CAVs can effectively reduce the queue length at signalized intersections and improve the intersection capacity. The abovementioned research demonstrates that CA models can be widely applied to traffic flow studies to reproduce the actual traffic characteristics.

The scholars mentioned above have primarily concentrated on investigating the driving characteristics of individual vehicles within mixed traffic flow, thereby inadvertently neglecting the interactive dynamics among CAVs. With the evolution of vehicular networking technology, CAVs synchronize their driving states with preceding vehicles through real-time communication facilitated by V2V and V2X technologies, culminating in forming platoons with a lead vehicle. Such CAV platoons typically comprise multiple trailing vehicles, thereby maintaining smaller headways within the platoon, which can substantially enhance road capacity [37]. Building upon this premise, Wu et al. [38] considered CAV platoons and developed a greedy algorithm-based cellular automaton model for interactions in a connected vehicle environment. The CAV platoons are regarded as the fundamental control element in this model. To pass through the intersection, the platoons cooperate and communicate with each other. However, the only vehicles involved in the traffic flow in this study are CAVs, and the primary responsibility of the CAV platoons is to regulate them as the fundamental unit when crossing the intersection. Yangsheng et al. [39] further considered degraded car-following in mixed traffic flow. They categorize vehicles on the road into distinct car-following modes based on their driving characteristics. Particularly, vehicles coalesce into platoons under the CACC car-following mode. The study revealed that when the penetration rate reaches 100%, all CAVs on the road travel in platoons, with road capacity being solely influenced by the critical density. However, it is noteworthy that the study did not account for platoon size limitations, leading to a discrepancy between actual and calculated capacity.

Based on the abovementioned research, it can be found that the existing studies have not sufficiently addressed the impact of platoon size on mixed traffic flows. When one platoon reaches its maximum size, the following CAVs will form a new platoon. Few scholars have studied the car-following behavior between two platoons. This paper establishes a cellular automaton model for interplatoon and intraplatoon car-following and determines the optimal platoon size under different traffic densities.

3. Methodology

3.1. Car-Following Mode. Amidst the ongoing advancements in intelligent connected technology, it is common to witness CAVs traveling in platoons within mixed traffic

flows. These platoons typically comprise a leading vehicle and one or more following vehicles. Figure 1 visually shows the four different car-following patterns that can be observed in a mixed traffic flow.

3.1.1. Human-Driven Vehicle Mode. As indicated in Figure 1, when the ego vehicle is an HDV, regardless of whether the preceding vehicle is an HDV or a CAV, the ego vehicle adopts the HDV car-following mode. In the traffic flow, when the driving behavior of the preceding vehicle changes, the ego vehicle needs some time to determine the changes in the preceding vehicle's behavior and take corresponding measures. For the convenience of description, this time is referred to as the reaction time in this paper. For the HDV car-following mode, the reaction time depends on individual differences between the drivers. By considering factors such as the driver's age, personality, and driving behavior, the speed of HDVs undergoes a random deceleration process, which is referred to as the random slowdown process in this paper.

3.1.2. Adaptive Cruise Control Mode. When the ego vehicle is a CAV, and the preceding vehicle is an HDV, this car-following mode is known as the ACC mode. In this mode, the ego vehicle cannot communicate directly with the preceding vehicle. However, it can leverage communication with the roadside infrastructure to acquire real-time information regarding the driving behavior of the preceding vehicle and respond promptly. The response time in this scenario is contingent upon the processing time of the onboard system for handling the received information and it is shorter compared to the reaction time in the HDV mode.

3.1.3. Cooperative Adaptive Cruise Control Mode. In the CACC car-following mode, the ego and the preceding vehicles are CAVs. In this mode, the ego vehicle can quickly perceive the driving state changes of the preceding vehicle through real-time communication between vehicles and adjust its driving behavior to maintain consistency with the preceding vehicle, thus forming a platoon. However, CAV platoons usually have a certain size limit (S is the maximum platoon size). When a platoon is full, and the $S+1$ vehicle is a CAV, it will lead another platoon on the road. At this point, the car-following mode between the $S+1$ vehicle and the preceding platoon is the intraplatoon car-following mode, while the car-following mode between the remaining vehicles is the interplatoon car-following mode. This study reflects the main differences between the two car-following modes in the reaction time and the rules of acceleration and deceleration.

3.2. Mixed Traffic Flow Cellular Automaton Model

3.2.1. Safe Distance. As shown in Figure 2, this paper introduces the concept of safe distance and defines it as the minimum distance required to prevent a collision with the preceding vehicle when the preceding vehicle brakes suddenly. The safe distance is defined as follows:

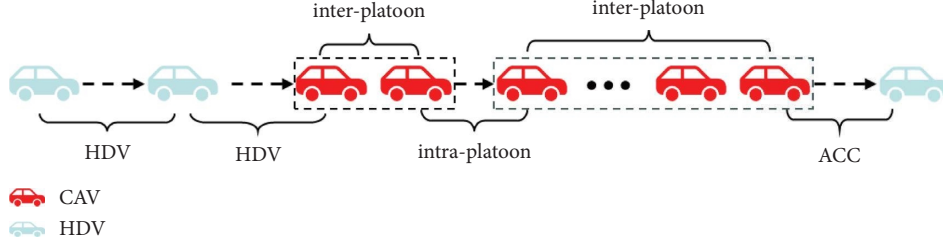


FIGURE 1: The diagram of the car-following models.

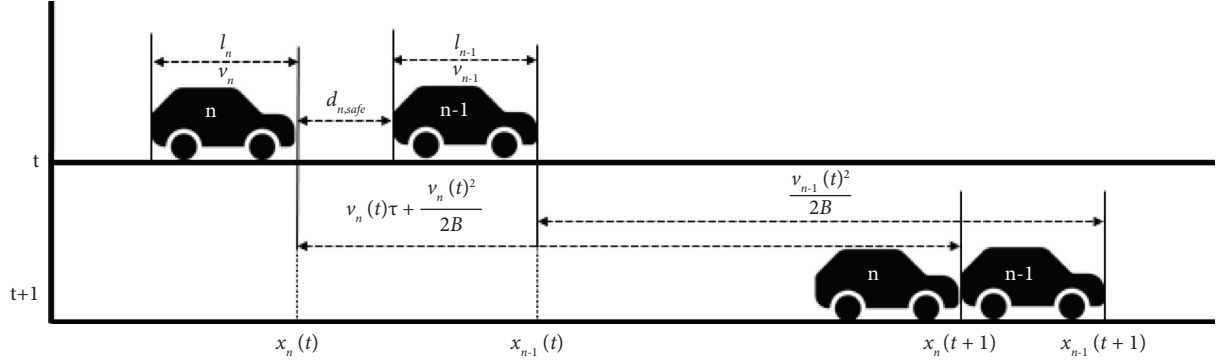


FIGURE 2: Safety distance diagram.

$$d_{n,\text{safe}} = v_n(t)\tau + \frac{v_n(t)^2 - v_{n-1}(t)^2}{2B}, \quad (1)$$

where $d_{n,\text{safe}}$ is the minimum safe distance between the vehicle n and $n-1$, $v_n(t)$ and $v_{n-1}(t)$ are the velocities of vehicle n and vehicle $n-1$ at time t , respectively, B is the maximum deceleration of the vehicle, and τ is the reaction time of the vehicle.

3.2.2. HDV- and ACC-Following Modes. The ego and preceding vehicles cannot exchange information in HDV and ACC modes. Only the difference in reaction time must be considered in the modeling. Therefore, this paper models the abovementioned two modes together.

(1) Acceleration

In actual traffic, when road conditions are favorable, and visibility is excellent, vehicles frequently accelerate to maximize travel efficiency. For the HDV and ACC modes, when the distance between the preceding vehicle and the ego vehicle exceeds the safety distance, the following vehicle will accelerate, according to the following equation:

$$v_n(t+1) = \min(v_n(t) + a_n, v_{\max}, d_n), d_n > d_{n,\text{safe}}, \quad (2)$$

where $v_n(t+1)$ is the velocity of the vehicle n at time $t+1$, a_n is the acceleration of the vehicle, v_{\max} is the maximum velocity of the vehicle, $d_n = x_{n-1} - x_n - l$ is the distance between the vehicle n and the vehicle $n-1$, x_{n-1} and x_n are the positions of the vehicle n and the vehicle $n-1$ at time t , l is the length of the vehicle, and $d_{n,\text{safe}}$ is the secure distance between the

vehicle n and the vehicle $n-1$. According to equation (1), this parameter's value depends on the reaction time, which differs between HDV and ACC modes. Consequently, the difference between HDV and ACC modes is reflected in the option of the reaction time utilized in the safe distance calculation.

(2) Deceleration

To ensure driving safety, the vehicle will decelerate when the distance between vehicle n and the preceding vehicle $n-1$ is less than or equal to the safe distance. The specific regulation is as follows:

$$v_n(t+1) = \min(v_n(t), d_n), d_n \leq d_{n,\text{safe}}. \quad (3)$$

Equation (3) indicates that when d_n is less than $d_{n,\text{safe}}$, the vehicle will decelerate to d_n to ensure secure driving; when d_n is equal to $d_{n,\text{safe}}$, it will maintain a constant speed while ensuring safety. As with the acceleration rule, the difference between HDV and ACC modes resides in the response time.

(3) Random deceleration

Due to the impact of personal factors such as age, gender, and temperament on driving behavior, random deceleration may occur during the driving process. Typically, equation (4) represents the specific rule that vehicles in motion are generally subject to random slowdown with a certain probability p_{slow} , i.e.,

$$v_n(t+1) = \max(v_n(t) - b_n, 0), \quad (4)$$

where b_n is the random deceleration of vehicle n . Specifically, since CAVs are not affected by the

driver's actions, the ACC mode does not account for sporadic deceleration.

(4) Position update

After updating the speed, the vehicle's position is updated according to equation (5).

$$x_n(t+1) = x_n(t) + v_n(t+1). \quad (5)$$

3.2.3. Intraplatoon-Following Mode

(1) Velocity update

Under the intraplatoon mode, acceleration driving can be initiated if either of the following two conditions is met: (a) when the distance between the ego vehicle and the preceding vehicle exceeds the safety distance, the ego vehicle will accelerate; (b) considering the intraplatoon mode with intervehicle communication, even if the distance between the ego vehicle and the preceding vehicle is less than the safe distance, it is considered to be safe when the speed of the preceding vehicle is greater than the speed of the ego vehicle.

When the safety gap between the ego vehicle and the preceding vehicle is less than or equal to the safety distance, and the preceding vehicle's speed is less than the ego vehicle's speed, the vehicle will decelerate.

To better describe the speed change circumstance, this article introduces the concept of expected speed to characterize these two acceleration rules, as shown in equation (6).

$$v_{s,n}(t) = \begin{cases} v_n(t) + a, & d_n > d_{n,\text{safe}}, \\ v_n(t) + a \cdot \text{sgn}(v_{n-1}(t) - v_n(t)), & d_n \leq d_{n,\text{safe}}, \end{cases} \quad (6)$$

where $\text{sgn}(X)$ is the speed judgment function, and the exact value is represented by equation (7).

$$\text{sgn}(X) = \begin{cases} 1, & X > 0, \\ 0, & X \leq 0. \end{cases} \quad (7)$$

Using equations (6) and (7), we can derive the intraplatoon mode speed update rule shown in equation (8).

$$v_n(t+1) = \min(v_{s,n}(t), d_n, v_{\max}). \quad (8)$$

(2) Position update

In the intraplatoon mode, the equation for updating the vehicle's location is given in equation (5).

3.2.4. Interplatoon Following Mode. When the vehicle's following mode is interplatoon, the ego vehicle can constantly travel in a convoy with the preceding vehicle. All

vehicles in the convoy maintain the same pace and driving style. This paper simulates it from two perspectives: before the formation of CAV platoons and after the formation of CAV platoons.

(1) Before the formation of CAV platoons

Before forming a platoon, the distance between the ego vehicle and the preceding vehicle is greater than the safe distance, indicating good road conditions. Under the CACC mode, the ego vehicle can synchronize with the preceding vehicle's state changes through V2V communication, enabling the ego vehicle to accelerate and form a platoon with the preceding vehicle as quickly as possible. The specific acceleration rules are as follows:

$$v_n(t+1) = \min(v_n(t) + a, v_{\max}, v_{n-1}(t) + d_n - d_{n,\text{safe}}) \cdot d_n > d_{n,\text{safe}}, \quad (9)$$

where $v_{n-1}(t) + d_n - d_{n,\text{safe}}$ is the following process of vehicle n under interplatoon mode from state $d_n > d_{n,\text{safe}}$ to state $d_n = d_{n,\text{safe}}$.

(2) After the formation of CAV platoons

When the ego vehicle accelerates, the distance between the ego vehicle and the preceding vehicle equals the safe distance, and the two vehicles will merge into a platoon and proceed together. Once the platoon is established, both vehicles will adopt the same driving behavior, by adhering to the specific evolution rules.

$$v_n(t+1) = v_n(t), d_n = d_{n,\text{safe}}. \quad (10)$$

(3) Position update

In the interplatoon mode, the equation for updating the vehicle's location is given in equation (5).

3.3. Theoretical Traffic Capacity Calculation. Traffic capacity refers to the maximum number of vehicles traversing a given stretch of road in each period under specified road conditions. This paper computes the traffic capacity by using the average headway time. When the CAV penetration rate is p ($0 < p < 1$), the HDV penetration rate is $1 - p$. If the vehicles are independent of each other, then $p - p^2$ can be used to calculate the proportion of ACC. By referring to [40], it is possible to calculate the probabilities of intraplatoon and interplatoon. When the traffic flow is stable and vehicle velocities are equivalent, the average headway \bar{h} can be calculated as follows:

$$\bar{h} = (1-p)\tau_{\text{HDV}} + p(1-p)\tau_{\text{ACC}} + \frac{(1-p)p^{S+1}}{1-p^S}\tau_{\text{LC}} + \frac{p^2(1-p^{S-1})}{1-p^S}\tau_{\text{FC}}, \quad (11)$$

where τ_{HDV} , τ_{ACC} , τ_{LC} , and τ_{FC} are the reaction times of HDV, ACC, intraplatoon, and interplatoon, respectively. By substituting equation (11) into the equation for calculating the road capacity $C = 3600/\bar{h}$, we can obtain

$$C = \frac{3600}{(1-p)\tau_{HDV} + p(1-p)\tau_{ACC} + ((1-p)p^{S+1}/1-p^S)\tau_{LC} + (p^2(1-p^{S-1})/1-p^S)\tau_{FC}}, 0 \leq p < 1. \quad (12)$$

When the CAV penetration rate reaches 100%, vehicles on the road form platoons, with each platoon consisting of one vehicle in the intraplatoon mode and $S-1$ vehicles in the interplatoon mode. When the traffic flow reaches a stable state, the average headway can be calculated as follows:

$$\bar{h} = \frac{(S-1)\tau_{FC} + \tau_{LC}}{S}. \quad (13)$$

By substituting equation (13) into the equation for calculating the road capacity $C = 3600/\bar{h}$, we can obtain

$$C = \frac{3600S}{(S-1)\tau_{FC} + \tau_{LC}}, p = 1. \quad (14)$$

In summary, the following equation is used to calculate the theoretical traffic capacity:

$$C = \begin{cases} \frac{3600}{(1-p)\tau_{HDV} + p(1-p)\tau_{ACC} + ((1-p)p^{S+1}/1-p^S)\tau_{LC} + (p^2(1-p^{S-1})/1-p^S)\tau_{FC}}, 0 \leq p < 1, \\ \frac{3600S}{(S-1)\tau_{FC} + \tau_{LC}}, p = 1. \end{cases} \quad (15)$$

4. Numerical Analysis

4.1. Simulation Environment Setup. This paper concentrates on the single-lane highway as the subject of its investigation. The lane consists of 4,000 cells, each measuring 1 meter in length. Therefore, the length of the road is 4000 meters. The simulation is conducted with periodic boundary conditions, a one-second time step, and four thousand cumulative steps. The data collected after stabilized traffic flow (2,000 seconds) will be analyzed as simulation results. Each car has a random speed and is evenly distributed on the road in the initial condition. The vehicle's maximum speed has been set to 35 m/s (126 km/h), and its conventional acceleration and random deceleration have been set to 2 m/s² and 3 m/s². The maximum deceleration B is set to 5 m/s², vehicle length is 5 m, and reaction times τ_{HDV} , τ_{ACC} , τ_{FC} , and τ_{LC} are, respectively, set to 2 s, 1.5 s, 1 s, and 0.4 s. The probability of random stalling P_{slow} is 0.3. To enhance the precision of the results, each simulation group is executed 10 times with different random speeds, and the final average value is recorded.

4.2. Simulation Result Analysis

4.2.1. Analysis of the Basic Traffic Flow Diagram. Figure 3 depicts the density-flow-speed fundamental diagram for various CAV penetration rates when $S=6$. As shown in Figure 3(a), when the CAV penetration rate remains constant, the average speed remains constant as the density increases and then starts to decrease. This indicates that

vehicles can maintain high-speed driving in free-flow conditions, and the introduction of CAVs has little impact on traffic flow. However, an increase in the CAV penetration rate alleviates traffic congestion in congested flow conditions. When the CAV penetration rate reaches 100%, it can maintain high speed at a vehicle density of 60 veh/km. As demonstrated in Figure 3(b), the density range of the free-flow phase varies at different penetration rates. A higher CAV penetration rate leads to a wider density range in the free-flow stage than a lower CAV penetration rate. This can be attributed to the superior performance of CAVs compared to the conventional vehicles. A larger free-flow phase indicates a higher capacity. As the CAV penetration rate increases, the road capacity consistently improves. At a CAV penetration rate of 60%, the road capacity is 1.6 times that of purely HDVs. When the CAV penetration rate reaches 80%, the road capacity increases to 2.2 times to that of purely HDVs. When the penetration rate reaches 100%, the road capacity is amplified to 4.3 times to that of purely HDVs. This is because CAVs do not undergo random slowdown processes and can adjust their speed to form platoons with preceding vehicles quickly. Once a platoon is formed, vehicles within the platoon travel at the same speed, thereby significantly improving the road space utilization. Hence, CAVs play a crucial role in enhancing the road capacity.

To verify the accuracy of the simulation model, this paper calculates the theoretical traffic capacity by substituting the platoon size $S=6$ into equation [12] and compares it to the

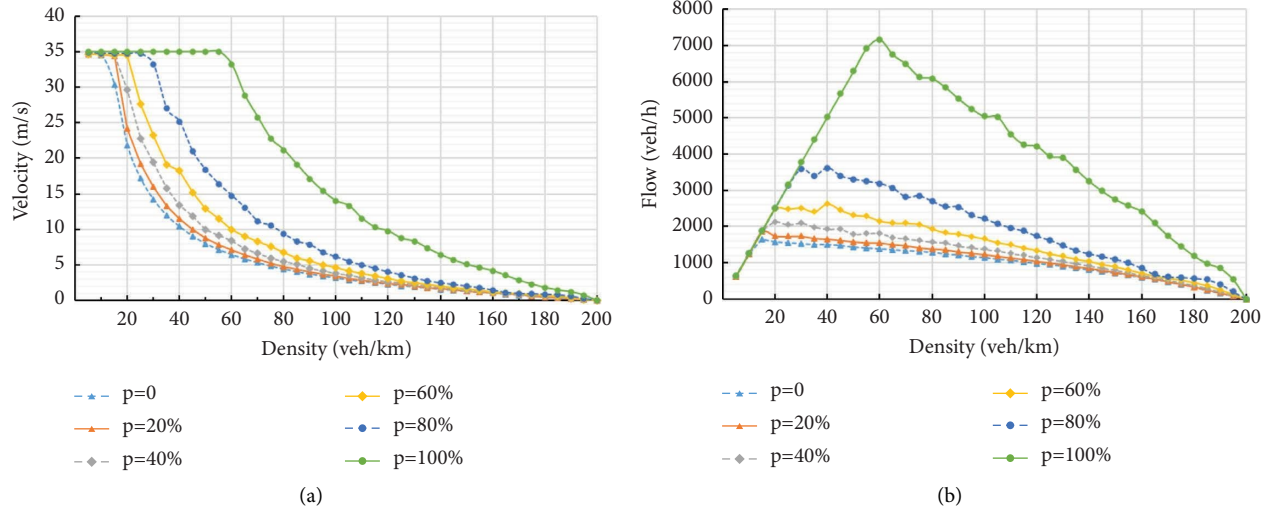


FIGURE 3: The fundamental diagram of mixed traffic flow under different penetration rates. (a) The fundamental velocity-density diagram. (b) The fundamental flow-density diagram.

simulation results shown in Table 1 to determine if the model is accurate. The error between the theoretical and simulation traffic capacity under differing CAV penetration rates is within 9%, and it is only 0.46% when the CAV penetration rate is 100%. Therefore, the model error in this paper is relatively small, and it can accurately simulate the actual road traffic situation.

4.2.2. Traffic Congestion Analysis. To quantitatively describe traffic congestion, this article uses the ratio of congested vehicles to reflect traffic congestion [31]. The equation for calculation is as follows:

$$CR = \frac{n}{\Delta TN}, \quad (16)$$

where ΔT is the simulation time step, N is the total number of vehicles, and n is the number of severely congested vehicles, which are those moving slower than 10 km/h on the roadway.

Figure 4 depicts the correlation between vehicle density and traffic congestion. The congestion rate progressively rises with increasing vehicle density. Nonetheless, the density threshold for congestion onset varies across different CAV penetration rates, whereby a higher CAV penetration rate indicates a higher threshold. At a CAV penetration rate of 0, congestion initiates at a density of 15 vehicles/km. At a penetration rate of 60%, congestion commences at a density of 25 veh/km. When the penetration rate reaches 100%, congestion emerges at a density of 150 vehicles/km. Meanwhile, at the same density, the higher the CAV penetration rate, the smaller the congestion ratio.

To delve deeper into this phenomenon, this study examines traffic congestion under different CAV penetration rates at a density of 100 veh/km, as presented in Table 2. The results highlight a significant reduction in the congestion rate as the CAV penetration rate increases. Specifically, compared to exclusively HDVs, the congestion rate decreases by 63.71%

TABLE 1: Comparison table of theoretical capacity and simulation.

Penetration rate	Theoretical capacity	Simulation capacity	Error (%)
0	1800	1639	8.94
0.2	1940	1890	2.56
0.4	2216	2130	3.88
0.6	2746	2630	4.22
0.8	3871	3624	6.37
1	7200	7167	0.46

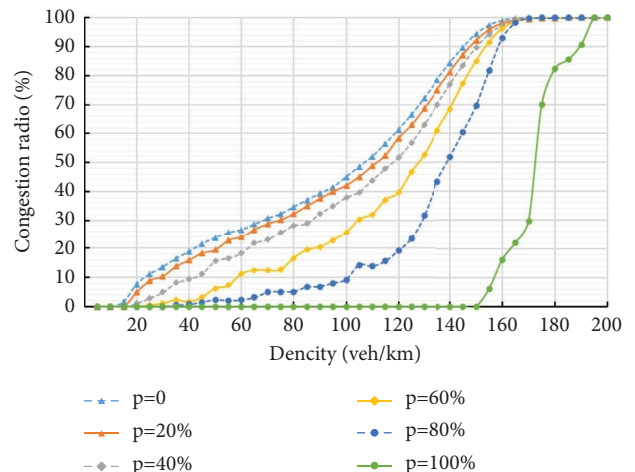


FIGURE 4: Traffic congestion analysis diagram.

at a CAV penetration rate of 80% and by 100% at a CAV penetration rate of 100%. This outcome is attributed to the diminished influence of random deceleration in HDVs in high CAV penetration rate scenarios. Moreover, the likelihood of vehicles forming stable platoons on the road increases, thereby contributing to higher average speeds and traffic congestion mitigation.

TABLE 2: Traffic congestion ratio analysis (100 vehicles/km).

Penetration rate (%)	Congestion rate (%)	Congestion reduction rate (%)
0	45.04	0.00
20	42.08	6.57
40	37.92	9.87
60	25.61	32.47
80	9.29	63.71
100	0.00	100.00

4.2.3. Analysis of the Maximum Vehicle Platoon. Figure 5 illustrates the influence of the maximum platoon length on road capacity. Traffic capacity increases as the maximum platoon length increases. This can be attributed to the greater number of vehicles operating in an interplatoon mode within the platoon, which decreases the average headway and enhances road capacity. However, factors beyond road capacity, such as communication range, platoon stability, and controllability, should be considered when determining the optimal platoon size. A larger platoon size necessitates a wider communication range and a more resilient control strategy. Hence, a larger platoon size is not always advantageous, as other factors must be considered.

To determine the optimal platoon size at various vehicle densities, this study divides the vehicle densities into three sections. The relationship between traffic flow and platoon size for these densities is depicted in Figure 6.

In the first section, a density of 20 vehicles/km is chosen to investigate the impact of the maximum platoon size on traffic flow. The blue line in Figure 6 indicates that, at this vehicle density, the influence of the platoon size on traffic flow is little. This can be attributed to the low vehicle density, where vehicles are in a state of free flow. Although platoon size affects the average headway, the vehicle speed remains constant, resulting in negligible changes in traffic flow.

Moving to the second section, a density of 60 vehicles/km is selected. The orange line in Figure 6 reveals that the traffic flow gradually increases and stabilizes as the platoon size increases from 2 to 7 vehicles. This suggests that, in this particular scenario, a platoon size of 7 vehicles is optimal. This is because when the platoon size is between 2 and 7 vehicles, more platoons are on the road, meaning more vehicles are in the intraplatoon mode. Compared to vehicles in the interplatoon mode, vehicles in the intraplatoon mode require a larger safety distance. Due to the high vehicle density in this scenario and the short distances between platoons, the intraplatoon mode's safety distance requirement cannot be met, leading to deceleration. As the platoon size increases, the number of vehicles in the intraplatoon mode decreases, resulting in fewer decelerations between platoons and an overall increase in traffic flow. When the platoon size reaches or exceeds 7, all vehicles in this scenario achieve a free flow state, causing the traffic flow to remain unchanged despite further increases in platoon size.

In the third section, a density of 100 vehicles/km is employed. The gray line in Figure 6 demonstrates that, in this scenario, the traffic flow increases with larger platoon sizes. This is due to the high vehicle density, which makes it challenging to attain a free-flow state. The average headway decreases as the platoon size increases, thereby improving the traffic flow.

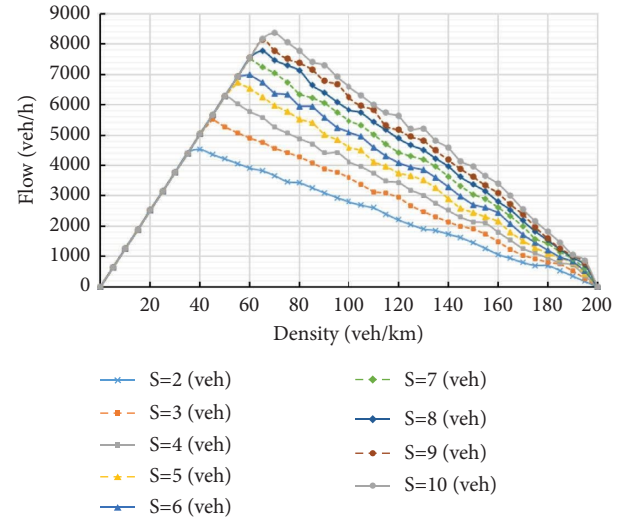


FIGURE 5: Analysis diagram of fleet size sensitivity.

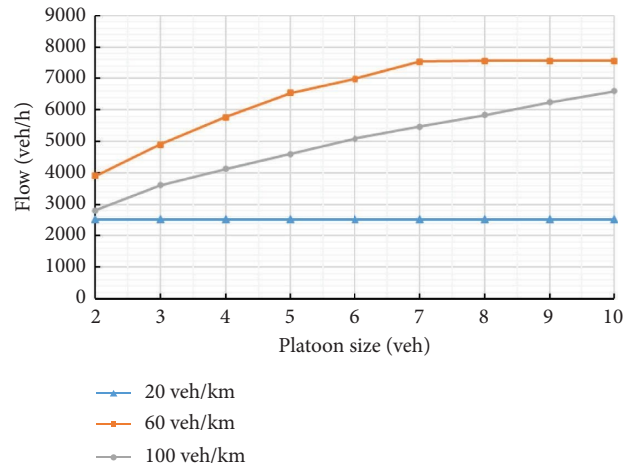


FIGURE 6: Plot of traffic versus fleet size for different vehicle densities.

4.2.4. Analysis of the Response Time of HDV and Interplatoon. Human drivers impact the response time of HDV, whereas the system's communication time determines the response time of interplatoon. In the sensitivity analysis, the density is set to 40 vehicles/km, where the τ_{HDV} varies from 1.8 s to 2.4 s with a 0.1 s increment and τ_{FC} varies from 0.3 s to 0.6 s with a 0.05 s increment. The results of the sensitivity analysis are depicted in Figure 7.

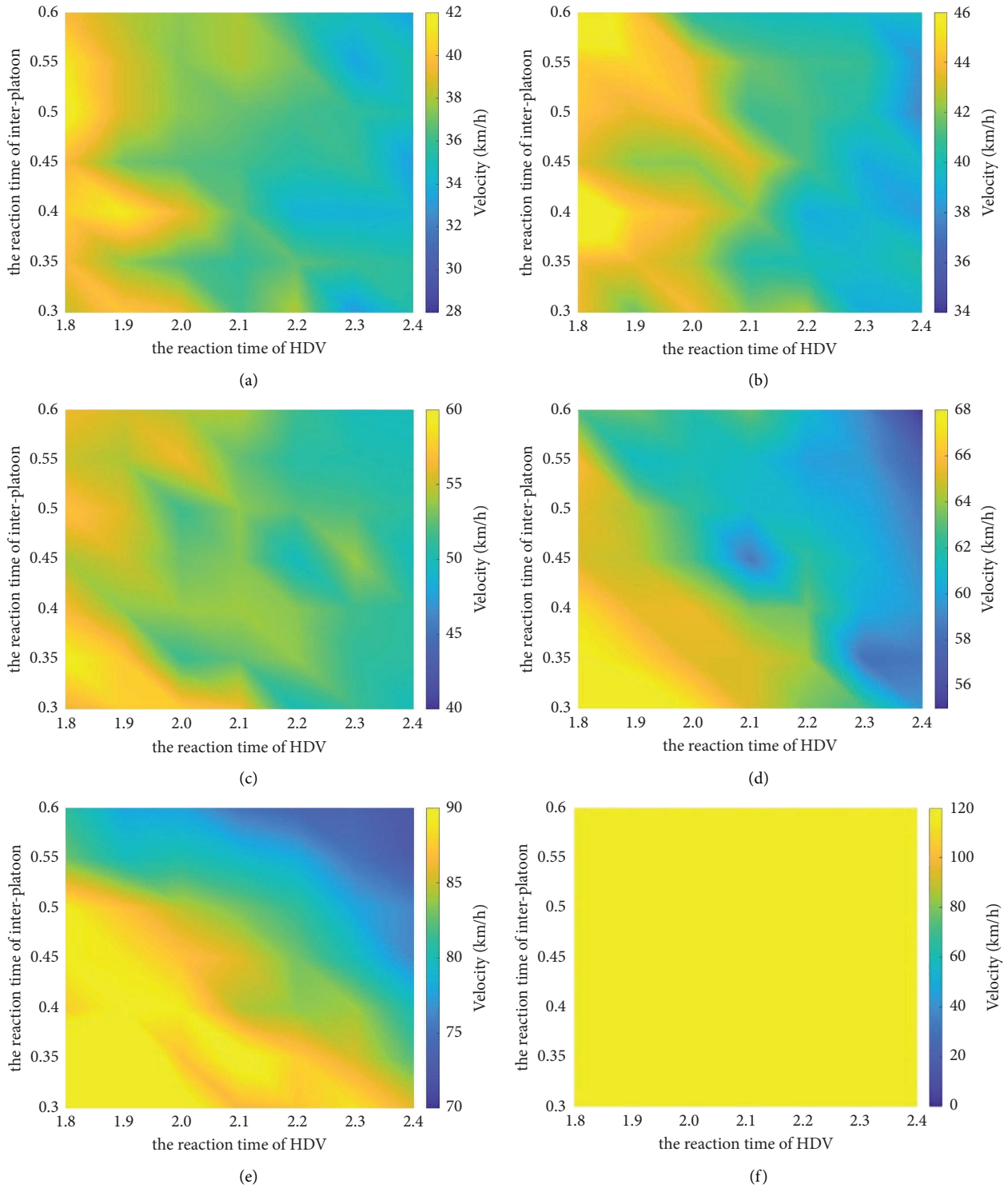


FIGURE 7: Sensitivity analysis of response time for HDV and interplatoon. (a) $p = 0\%$. (b) $p = 20\%$. (c) $p = 0\%$. (d) $p = 20\%$. (e) $p = 0\%$. (f) $p = 20\%$.

Figure 7 illustrates notable disparities in the influence of τ_{HDV} and τ_{FC} on average speed at varying CAV penetration rates. Regarding HDVs, an augmented reaction time among different CAV penetration rates leads to a substantial decline in the average speed. Equation (1) reveals that an increased human driver reaction time

necessitates a larger safety distance. Consequently, under the speed update rule for HDVs, there is a reduction in the number of vehicles opting for acceleration in the subsequent time step, accompanied by a corresponding increase in deceleration choices, resulting in a decreased average speed.

Concerning CAVs, under low CAV penetration rates (Figures 7(a)–7(c)), the average speed remains unaffected by τ_{FC} . This arises due to the dominance of HDVs at low CAV penetration rates, resulting in a scarcity of vehicles forming the interplatoon mode on the road. Consequently, the impact of τ_{FC} is little. However, under high CAV penetration rates (Figures 7(d) and 7(e)), as τ_{FC} increases, the average speed decreases substantially.

5. Conclusion

This study considers the limitation of the platoon size and categorizes vehicles in a mixed traffic flow into four types: HDV, ACC, interplatoon, and intraplatoon. By employing numerical simulations, the analysis focuses on traffic characteristics, congestion levels, and reaction times across varying CAV penetration rates. The investigation aims to determine the optimal platoon size under different traffic densities, leading to the following key findings:

- (1) CAVs make substantial improvements in road capacity. Compared to pure HDVs, a penetration rate of 80% enhances the road capacity by 2.2 times, while a 100% penetration rate results in a 4.3-fold increase.
- (2) Traffic flow experiences a continuous decrease in average speed as the density rises. However, under the same density, the average speed of the vehicles increases with higher penetration rates.
- (3) Congestion levels escalate with increased vehicle densities. Nonetheless, higher CAV penetration rates effectively alleviate road congestion at the same vehicle density, with a particularly pronounced reduction observed when the CAV penetration rate surpasses 60%.
- (4) At a 100% CAV penetration rate, road capacity expands with larger platoon sizes. However, an optimal platoon size exists for a specific vehicle density.
- (5) HDV vehicles exhibit a significant reduction in average speed with increasing τ_{HDV} under different penetration rates. Similarly, interplatoon vehicles experience a notable average speed decrease with growing τ_{FC} at high CAV penetration rates.

This study primarily distinguishes between CAVs and HDVs. In future investigations, further subdivision into passenger cars, trucks, and small cars, while considering distinct characteristics among vehicles and driver behavior, would enable the development of a comprehensive mixed traffic flow model to validate the traffic characteristics in real-world scenarios. In addition, it is noteworthy that this study's analysis of optimal platoon size solely accounts for its impact on road capacity. Subsequent research endeavors could explore factors such as platoon stability and controllability.

Data Availability

The data used to support the findings of this study are included within the article.

Conflicts of Interest

The authors declare that they have no conflicts of interest.

Acknowledgments

The paper received research funding support from the Fundamental Research Funds for the Central Universities (2682023ZTPY034), the Chengdu Soft Science Research Project (2023-RK00-00029-ZF), and the Education Department of Hunan Province (20A009).

References

- [1] A. Talebian and S. Mishra, "Predicting the adoption of connected autonomous vehicles: a new approach based on the theory of diffusion of innovations," *Transportation Research Part C: Emerging Technologies*, vol. 95, pp. 363–380, 2018.
- [2] Z. Yao, T. Xu, Y. Jiang, and R. Hu, "Linear stability analysis of heterogeneous traffic flow considering degradations of connected automated vehicles and reaction time," *Physica A: Statistical Mechanics and Its Applications*, vol. 561, Article ID 125218, 2021.
- [3] D. Chen, S. Ahn, M. Chitturi, and D. A. Noyce, "Towards vehicle automation: roadway capacity formulation for traffic mixed with regular and automated vehicles," *Transportation Research Part B: Methodological*, vol. 100, pp. 196–221, 2017.
- [4] Y. Jiang, B. Zhao, M. Liu, and Z. Yao, "A two-level model for traffic signal timing and trajectories planning of multiple CAVs in a random environment," *Journal of Advanced Transportation*, vol. 2021, Article ID 9945398, 13 pages, 2021.
- [5] Z. Yao, R. Hu, Y. Jiang, and T. Xu, "Stability and safety evaluation of mixed traffic flow with connected automated vehicles on expressways," *Journal of Safety Research*, vol. 75, pp. 262–274, 2020.
- [6] J. Lioris, R. Pedarsani, F. Y. Tascikaraoglu, and P. Varaiya, "Platoons of connected vehicles can double throughput in urban roads," *Transportation Research Part C: Emerging Technologies*, vol. 77, pp. 292–305, 2017.
- [7] J. Axelsson, "Safety in vehicle platooning: a systematic literature review," *IEEE Transactions on Intelligent Transportation Systems*, vol. 18, no. 5, pp. 1033–1045, 2017.
- [8] M. Balac, S. Hörll, and K. W. Axhausen, "Fleet sizing for pooled (automated) vehicle fleets," *Transportation Research Record: Journal of the Transportation Research Board*, vol. 2674, no. 9, pp. 168–176, 2020.
- [9] M. Sala and F. Soriguera, "Capacity of a freeway lane with platoons of autonomous vehicles mixed with regular traffic," *Transportation Research Part B: Methodological*, vol. 147, pp. 116–131, 2021.
- [10] M. Sala and F. Soriguera, "Macroscopic modeling of connected autonomous vehicle platoons under mixed traffic conditions," *Transportation Research Procedia*, vol. 47, pp. 163–170, 2020.
- [11] K. Bentaleb, N. Lakouari, H. Ez-Zahraouy, and A. Benyoussef, "Simulation study of satisfaction rate in the mixed traffic flow with open boundary conditions," *International Journal of Modern Physics C*, vol. 27, no. 02, Article ID 1650023, 2016.
- [12] X. Chang, X. Zhang, H. Li, C. Wang, and Z. Liu, "A survey on mixed traffic flow characteristics in connected vehicle environments," *Sustainability*, vol. 14, no. 13, Article ID 7629, 2022.
- [13] Y. Huang, D. Li, and J. Cheng, "Simulation of pedestrian–vehicle interference in railway station drop-off area

- based on cellular automata,” *Physica A: Statistical Mechanics and Its Applications*, vol. 579, Article ID 126142, 2021.
- [14] D. Kong, L. Sun, J. Li, and Y. Xu, “Modeling cars and trucks in the heterogeneous traffic based on car-truck combination effect using cellular automata,” *Physica A: Statistical Mechanics and Its Applications*, vol. 562, Article ID 125329, 2021.
- [15] X. Li, X. Li, Y. Xiao, and B. Jia, “Modeling mechanical restriction differences between car and heavy truck in two-lane cellular automata traffic flow model,” *Physica A: Statistical Mechanics and Its Applications*, vol. 451, pp. 49–62, 2016.
- [16] X. Chang, H. Li, J. Rong, X. Zhao, and A. Li, “Analysis on traffic stability and capacity for mixed traffic flow with platoons of intelligent connected vehicles,” *Physica A: Statistical Mechanics and Its Applications*, vol. 557, Article ID 124829, 2020.
- [17] Y. Jiang, S. Wang, Z. Yao, B. Zhao, and Y. Wang, “A cellular automata model for mixed traffic flow considering the driving behavior of connected automated vehicle platoons,” *Physica A: Statistical Mechanics and Its Applications*, vol. 582, Article ID 126262, 2021.
- [18] K. Ma, H. Wang, and T. Ruan, “Analysis of road capacity and pollutant emissions: impacts of connected and automated vehicle platoons on traffic flow,” *Physica A: Statistical Mechanics and Its Applications*, vol. 583, Article ID 126301, 2021.
- [19] J. Zhou and F. Zhu, “Analytical analysis of the effect of maximum platoon size of connected and automated vehicles,” *Transportation Research Part C: Emerging Technologies*, vol. 122, Article ID 102882, 2021.
- [20] Y. Jiang, T. Ren, Y. Ma, Y. Wu, and Z. Yao, “Traffic safety evaluation of mixed traffic flow considering the maximum platoon size of connected automated vehicles,” *Physica A: Statistical Mechanics and Its Applications*, vol. 612, Article ID 128452, 2023.
- [21] Z. Yao, Y. Wang, B. Liu, B. Zhao, and Y. Jiang, “Fuel consumption and transportation emissions evaluation of mixed traffic flow with connected automated vehicles and human-driven vehicles on expressway,” *Energy*, vol. 230, Article ID 120766, 2021.
- [22] K. Nagel and M. Schreckenberg, “A cellular automaton model for freeway traffic,” *Journal de Physique I*, vol. 2, no. 12, pp. 2221–2229, 1992.
- [23] M. Takayasu and H. Takayasu, “ $1/f$ noise in a traffic model,” *Fractals*, vol. 1, no. 4, pp. 860–866, 1993.
- [24] J. Zeng, S. Yu, Y. Qian, and X. Feng, “Expressway traffic flow model study based on different traffic rules,” *IEEE/CAA Journal of Automatica Sinica*, vol. 5, no. 6, pp. 1099–1103, 2018.
- [25] S. C. Benjamin, N. F. Johnson, and P. M. Hui, “Cellular automata models of traffic flow along a highway containing a junction,” *Journal of Physics A: Mathematical and General*, vol. 29, no. 12, pp. 3119–3127, 1996.
- [26] R. Barlovic, L. Santen, A. Schadschneider, and M. Schreckenberg, “Metastable states in cellular automata for traffic flow,” *The European Physical Journal B*, vol. 5, no. 3, pp. 793–800, 1998.
- [27] W. Knosp, L. Santen, A. Schadschneider, and M. Schreckenberg, “Towards a realistic microscopic description of highway traffic,” *Journal of Physics A: Mathematical and General*, vol. 33, no. 48, pp. L477–L485, 2000.
- [28] M. Fukui, Y. Ishibashi, and Yoshihiro, “Traffic flow in 1D cellular automaton model including cars moving with high speed,” *Journal of the Physical Society of Japan*, vol. 65, no. 6, pp. 1868–1870, 1996.
- [29] B. S. Kerner, S. L. Klenov, and D. E. Wolf, “Cellular automata approach to three-phase traffic theory,” *Journal of Physics A: Mathematical and General*, vol. 35, no. 47, pp. 9971–10013, 2002.
- [30] H. Emmerich and E. Rank, “An improved cellular automaton model for traffic flow simulation,” *Physica A: Statistical Mechanics and Its Applications*, vol. 234, no. 3-4, pp. 676–686, 1997.
- [31] D. Yang, X. Qiu, L. Ma, D. Wu, L. Zhu, and H. Liang, “Cellular automata-based modeling and simulation of a mixed traffic flow of manual and automated vehicles,” *Transportation Research Record: Journal of the Transportation Research Board*, vol. 2622, no. 1, pp. 105–116, 2017.
- [32] T. Vranken, B. Sliwa, C. Wietfeld, and M. Schreckenberg, “Adapting a cellular automata model to describe heterogeneous traffic with human-driven, automated, and communicating automated vehicles,” *Physica A: Statistical Mechanics and Its Applications*, vol. 570, Article ID 125792, 2021.
- [33] L. Ye and T. Yamamoto, “Evaluating the impact of connected and autonomous vehicles on traffic safety,” *Physica A: Statistical Mechanics and Its Applications*, vol. 526, Article ID 121009, 2019.
- [34] B. Gong, F. Wang, C. Lin, and D. Wu, “Modeling HDV and CAV mixed traffic flow on a foggy two-lane highway with cellular automata and game theory model,” *Sustainability*, vol. 14, no. 10, Article ID 5899, 2022.
- [35] R. Marzoug, N. Lakouari, H. Ez-Zahraouy, B. Castillo Téllez, M. Castillo Téllez, and L. Cisneros Villalobos, “Modeling and simulation of car accidents at a signalized intersection using cellular automata,” *Physica A: Statistical Mechanics and Its Applications*, vol. 589, Article ID 126599, 2022.
- [36] H. T. Zhao, X. R. Liu, X. X. Chen, and J. C. Lu, “Cellular automata model for traffic flow at intersections in internet of vehicles,” *Physica A: Statistical Mechanics and Its Applications*, vol. 494, pp. 40–51, 2018.
- [37] L. Zhao and J. Sun, “Simulation framework for vehicle platooning and car-following behaviors under connected-vehicle environment,” *Procedia- Social and Behavioral Sciences*, vol. 96, pp. 914–924, 2013.
- [38] W. Wu, Y. Liu, Y. Xu, Q. Wei, and Y. Zhang, “Traffic control models based on cellular automata for at-grade intersections in autonomous vehicle environment,” *Journal of Sensors*, vol. 2017, Article ID 9436054, 6 pages, 2017.
- [39] J. Yangsheng, W. Sichen, G. Kuan, L. Meng, and Y. Zhihong, “Cellular automata model of mixed traffic flow composed of intelligent connected vehicles’ platoon,” *Journal of System Simulation*, vol. 34, no. 5, 2022.
- [40] X. Chang, H. Li, J. Rong, Q. Lingqiao, and Y. Yanfang, *Analysis on Fundamental Diagram Model for Mixed Traffic Flow with Connected Vehicle Platoons*, Dongnan Daxue Xuebao (Ziran Kexue Ban)/Journal of Southeast University (Natural Science Edition), Mainland, China, 2020.